A Spectroscopic Study of the Classical Nova V723 Cassiopeia

A THESIS
SUBMITTED TO THE FACULTY OF THE GRADUATE SCHOOL
OF THE UNIVERSITY OF MINNESOTA
BY

Thomas John Vonderharr

IN PARTIAL FULFILLMENT OF THE REQUIREMENTS
FOR THE DEGREE OF
Master Of Science

Charles E. Woodward, Advisor

August, 2012

Acknowledgements

I would first like to thank my advisor, Dr. Charles (Chick) Woodward, for affording me the unique experiences I have encountered throughout my graduate school career. Few people are given the chance to see large astronomical observatories up close, and fewer still are those who get to use them in all their splendor.

In addition to Chick, I must also acknowledge the help and insights contributed by Dr. R. Mark Wagner over several visits to the University of Arizona as well as Mark visiting Minnesota. Dr. Greg Schwarz was also indispensable in aiding with X-ray observations, and Dr. Catrina Hamilton and her student K. A. Racine for their work with the photometry while I dealt with the spectral side of things.

Next I would like to thank L. Andrew Helton for training me in the art of astronomical observation, instrumentation, and data reduction, providing me with the skills I needed to carry out my thesis. I will never forget the nights spent at O'Brien Observatory splicing cables just to make an old computer mouse work and late night burger runs to Meister's, at Mount Lemmon debugging the broken declination motor, and our numerous runs to Kitt Peak and the associated late nights in Tucson as we prepared ourselves for the night schedule.

John Marchetti deserves mention for joining us at O'Brien and flying down to Arizona with Al Knutson on short notice to deliver a replacement motor for the broken one at Mount Lemmon, as well as being an outlet for my amateur astronomy interests and a source of many an interesting afternoon chat in the IR lab.

To Geno Bechetti, Dennis Means, and Mike Terenzoni—the telescope operators at the Bok 90" telescope—for their conversation and company during the long nights of observing on Kitt Peak, not to mention their professional services as well.

A huge thank you to Dinesh Shenoy for enduring the 28-hour/2-day drive each way

to and from Arizona with me, and the brief time we worked together on the MMTPol instrument and banging our heads against the broken MLOF motor culminating in the "million dollar screw".

Finally but by no means least: all the other graduate students who have not gotten individual mention here. Without them and their social support (a.k.a. Friday beers and July 4th camping trips), I may not have made it this far, and I certainly would not have as many stories to cherish.

Dedication

This work is dedicated to my wife, Becky, who has been a loving partner and an immense source of support throughout the entire process of earning my degree while taking on her own share of burdens. I could not have done it without her, and I look forward to many more years of post-graduate school life together.

Abstract

We have made observations of the classical nova V723 Cas over a period of 3 years (2007–2010) at a spectral resolution of ~ 2Å(125 km/s)in the wavelength range $\lambda\lambda$4180–5320Å, specifically targeting the emission lines He II λ4686 and Hβ λ4861. These observations were then compared to the system's periodic photometric behavior ($P \sim$ 16 hr, Goranskij et al. [2007]), assumed to correspond to the orbit of the binary pair. The purpose of the observations is to try and characterize the underlying star system of V723 Cas and determine why it has been a source of super-soft X-rays longer than any other nova on record, all in the context of whether classical novae are the true progenitors of type Ia supernovae.

For both lines, we detect periodic variability in the normalized intensity which is caused only by a changing intensity of the underlying continuum light. The level of continuum light over the entire period is consistent with the 1.6 magnitude amplitude of the light curve. Even accounting for this underpinning continuum light, the emission profiles of the two lines in question were seen to vary in radial velocity and/or intensity, especially so in Hβ. To account for the double-peaked profiles, we fit two models to the data: one using an accretion disk and the one using two independent, overlapping lines. Fits to the Hβ using an accretion disk yield a radial velocity curve 90° out of phase with the standard interpretation of a binary light curve, while the independent line approach yields systematic velocities that are blue-shifted when all other measurements indicate the system should have an overall redshift of ~ 100 km s^{-1}. The He II emission remains more of a mystery: whatever trends seem apparent by eye fail to be confirmed by both models which either do not converge to a solution or exhibit no obvious trend in the results.

In addition to the targeted emission lines, we also detected the presence of a blend of lines near He II in the range $\lambda\lambda$4640–4650. It is likely these lines arise due to the Bowen fluorescence mechanism and thus provide evidence of irradiation of the mass donor star in the nova binary. Gaussian fits to these lines constrain the orbital velocity of the secondary to $v_2 \sin i = 70 \pm 8$ km s^{-1} ($v_2 = 79 \pm 9$ km s^{-1} with $i = 62°$) that, contrary to the accretion disk fits for Hβ, are consistent with the typical light curve

interpretation. With no other spectral lines in our data shown conclusively to be in anti-phase with the Bowen lines, a similar measure on the primary star cannot be made at this time, and therefore a direct measurement of the mass ratio of the system also remains elusive.

Contents

List of Tables

List of Figures

Chapter 1

Introduction

1.1 Classical Novae

Classical novae (CNe; singular CN) are a class of binary star system consisting of a white dwarf (WD) primary star and a secondary star that is either a main sequence star or a star slightly evolved off the main sequence. The secondary star overfills its Roche lobe and mass and angular momentum are transferred to the WD via an accretion disk, building up a hydrogen-rich shell around the carbon and oxygen core which is supported against gravity by electron degeneracy pressure. When a sufficient amount of mass has built up and the temperature has reached a few million degrees, the base layers of the shell mix with the WD material and begin to fuse hydrogen into helium via the CNO cycle. Because the hydrogen-rich material at the base is now also degenerate, the pressure is independent of the temperature and the reaction cannot be slowed by the shell expanding and cooling. The reaction spreads rapidly in a thermonuclear runaway (TNR): the resulting brightening is seen as the nova explosion. The energy released by the TNR expels nuclear processed material and the upper layers of the accreted shell away from the system and forms a shell of ejecta that will eventually rejoin the interstellar medium. The WD core is not destroyed in the process and over time (hundreds to thousands of years) will accrete a new layer of hydrogen and the system may undergo repeated nova events. By definition, a CN has only a single observed outburst and when a second outburst is observed the system is reclassified as a recurrent nova (RN; plural RNe). Over sufficiently long timescales, all CNe are expected to become RNe.

While CNe are known for their explosive nature, observations carried out during the time of quiessence between outbursts also contains a wealth of information and can be used to study in detail the underlying binary nature and evolution of novae. The spectra of post-eruption novae display emission lines that can arise from many sources: the thinning nova ejecta, a re-established mass transfer stream from the secondary to the WD, the accretion disk, etc. If the spectra are taken with a short cadence relative to the orbital period of the system (typically $P_{orb} \sim$ few hours), the changing behavior of emission lines can distinguish between these possibilities and build up a physical picture of the binary system.

By understanding the behavior of novae in both eruption and quiescence, a larger question may also be answered: the source of the type Ia supernovae (SNe, singular SN). This special type of supernova has the distinction of having a bright and nearly constant luminosity, making it useful as a "standard candle" in making distance measurements of the farthest galaxies from Earth. It has long been postulated that this constancy is the result of a WD exceeding the $1.4M_{\odot}$ Chandrasekhar limit above which the star becomes too massive for electron degeneracy to support itself and therefore explodes. If CNe eject less mass than they accrete during each outburst, over time they could gain enough mass to exceed this limit and are thus a prime candidate for type Ia supernovae progenitor stars; a situation termed the 'single-degenerate case' (a second method that has been postulated is the collision and subsequent merging of two WDs into a single object, known as the 'double-degenerate case'). Whether or not it is common for CNe to gain mass post eruption is still an open question [Starrfield et al., 2012].

Verifying the single-degenerate case will give confidence in the use of type Ia SNe as true standard candles and the details of the progenitor systems may help explain the observed differences between individual SNe.

1.2 V723 Cassiopeia

The nova V723 Cas (Nova Cas 1995) was discovered on 1995 August 24 [Hirosawa et al., 1995] and reached maximum brightness of $V \sim 7$ mag in 1995 December. It then declined from maximum as one of the slowest novae on record, with a time to fade by 3 magnitudes of $t_3 \sim 173$ days [Chochol and Pribulla, 1997]. This decline time can

only be regarded as a rough estimate because of several sharp peaks of re-brightening in the optical light curve, including sharp peaking near the reported visual maximum. Excluding the outbursts and smoothing over small time-scale variations yields longer decline time estimates of $t_3 \sim 515$ days [Goranskij et al., 2007] and $t_3 \sim 778$ days [Evans et al., 2003]. Such large uncertainties make application of the maximum magnitude-rate of decline (MMRD) method problematic for determining the absolute magnitude of V723 Cas during the outburst. Following the initial eruption and decline V723 Cas has developed increasingly large periodic photometric variability in the optical and near-infrared. These asymmetric sinusoidal-like variations are attributed to the orbital motion of the binary system by Goranskij et al. [2007], who derive a period of 0.69327 days (16.6 hours) from the light curve.

In addition to its slow decline, V723 Cas has been an active super-soft X-ray source (SSS) for more than 15 years since its outburst in 1995 [Ness et al., 2008]. A recent survey of all novae known to have undergone an SSS phase reveals a median X-ray turn off time of only 1.4 years [Schwarz et al., 2011], drastically shorter than for V723 Cas which still has not turned off. Many novae are thought to experience the SSS phase due to residual nuclear burning of material on the surface of the white dwarf, especially those with high mass transfer rates from the secondary star. Mass loss from the outburst stifles the reactions, ending the SSS phase. Thus, the continued observation of super-soft X-ray emission from V723 Cas suggests that nuclear reactions may still be ongoing on the surface of the white dwarf (WD). One interesting possibility is that irradiation of the secondary star could be driving an enhanced mass transfer rate, providing a continuous fuel source to power the steady-state nuclear burning. This also elevates V723 Cas to the status of a candidate for the single-degenerate class of type Ia SN progenitors. It should be noted here that current models do not predict such steady-state burning to be possible [Woodward and Starrfield, 2011] given realistic parameters, complicating the possibility of V723 Cas as being a possible progenitor.

Unfortunately, the physical parameters of the V723 Cas system are poorly known other than the orbital period and, only recently, the distance and inclination. Lyke and Campbell [2009] using the OSIRIS integral field spectrograph[1] on the Keck II telescope were able to resolve the nova ejecta. The ejecta appear to be bipolar with an equatorial

[1] http://www2.keck.hawaii.edu/inst/osiris/

ring and—assuming the orbital plane coincides with the plane of the ejecta—indicate the V723 Cas system inclination to be $62\overset{\circ}{.}0 \pm 1\overset{\circ}{.}5$, ruling out disk eclipses as an explanation for the optical light curve. They also used expansion parallax to fix the system's distance at $3.85^{+0.23}_{-0.21}$ kpc, a figure that was previously a matter of contention due to the erratic light curve. A cartoon illustration of the possible structure of the system is presented in Figure 1.1 including the ejecta, WD, secondary star, accretion disk around the WD, a region on the secondary heated by the WD's high energy radiation, the mass transfer stream, and the "hot spot" where the stream impacts the disk. The mass of V723 Cas is notoriously poorly known. Estimates based on the t_3-WD mass relation of Livio [1992] are subject to the large uncertainty in t_3. Evans et al. [2003] use a value of $0.67 M_\odot$ based only on the mass of another nova, HR Del [Ritter and Kolb, 1998], which has a similar light curve to V723 Cas. Despite the difficulties in obtaining a numerical value for the mass, it is almost certain to be very low based on its slow speed class, nearing the limit of the minimum WD mass on which a nova eruption is even possible [Kovetz and Prialnik, 1985].

It is the goal of this thesis to put additional constraints on the V723 Cas system and understand what is causing the excessively long SSS state of this nova in the hope it may provide insight into determining the true progenitors of the type Ia SNe.

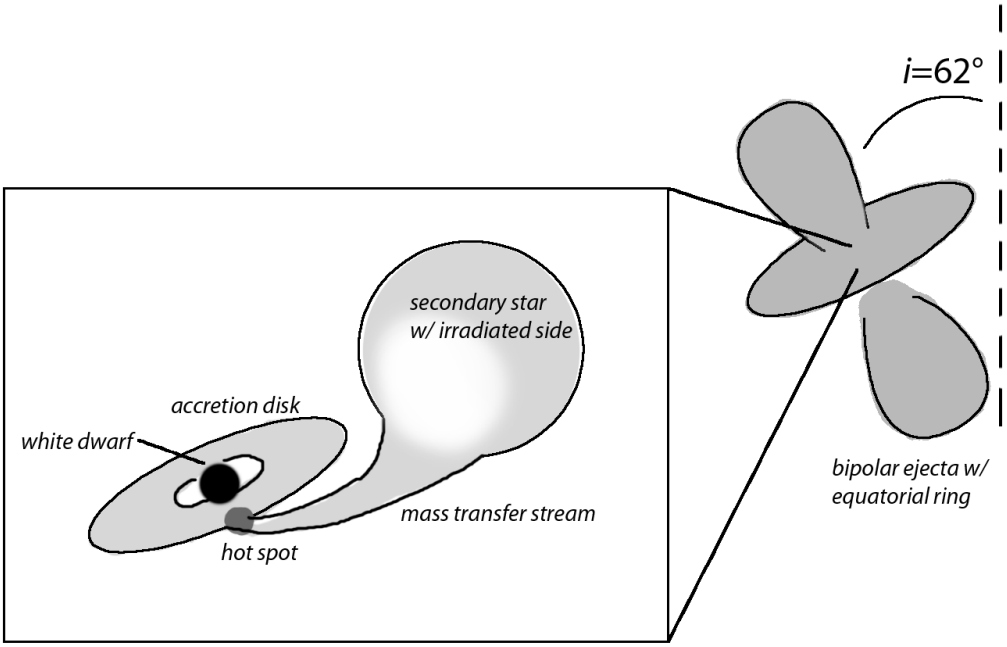

Figure 1.1 A cartoon illustration of the V723 Cas system showing its ejecta and the possible structures of the underlying binary system (inset).

Chapter 2

Observations

Our observations were carried out in 2007, 2008, and 2010 at a combination of the Steward Observatory Bok 90-inch (2.3-m) telescope with the Boller and Chivens Spectrograph[1] (B&C Spec) and the MDM Observatory Hiltner 2.4-m telescope with Modspec.[2] R.M. Wagner obtained the 2007 and 2008 data and the author obtained the additional 2010 data. We also attempted to acquire V723 Cas data in 2009 but were unable to get any images during that observing run. Table 2.1 lists the dates, spectral ranges, number of spectra taken, and range of orbital phases obtained. The spectral resolution of the data from both observatories is approximately $\sim$ 2Å. The exposure times for each image were 1200s in 2007 and 2008 and 1500s (5×300s) in 2010. These exposure times were chosen to be short compared with the 16.6 hour orbital period to minimize velocity smearing of features, with the increase in 2010 due to V723 Cas fading. An example spectrum with annotations for major features of relevance to this work is shown in Figure 2.1. To achieve higher signal-to-noise, the spectra were then co-added into ten bins in orbital phase (see Table 2.2) at the cost of some additional velocity smearing. The profiles of the two strongest emission lines (He II λ4686 and Hβ) are shown for each phase bin in Figure 2.2.

[1] `http://james.as.arizona.edu/~psmith/90inch/bcman/html/bcman.html`
[2] `http://www.astro.lsa.umich.edu/obs/mdm/technical/modular.html`

Table 2.1. Log of Observations

Date UT	Observatory	Range (Å)	No. Spectra	Phases[a]
2007 Oct 24	SO90[b]	4180–5320	14	0.31–0.64
2007 Oct 25	SO90	4180–5320	9	0.05–0.23
2008 Oct 16	MDM[c]	3900–5900	14	0.81–0.18
2010 Nov 13	SO90	4180–5320	8	0.17–0.42
2010 Nov 14	SO90	4180–5320	8	0.55-0.78

[a]Phase of the photometric light curve according to the ephemeris of Goranskij et al. [2007]

[b]Steward Observatory Bok 90-inch (2.3-m) telescope with B&C Spec

[c]MDM Observatory Hiltner 2.4-m telescope with Modspec

Table 2.2. Orbital Phases of the Spectra

Phases[a]	No. Spectra
0.0–0.1	6
0.1–0.2	9
0.2–0.3	5
0.3–0.4	7
0.4–0.5	5
0.5–0.6	6
0.6–0.7	5
0.7–0.8	3
0.8–0.9	4
0.9–1.0	3

[a]Phased according to the ephemeris of Goranskij et al. [2007]

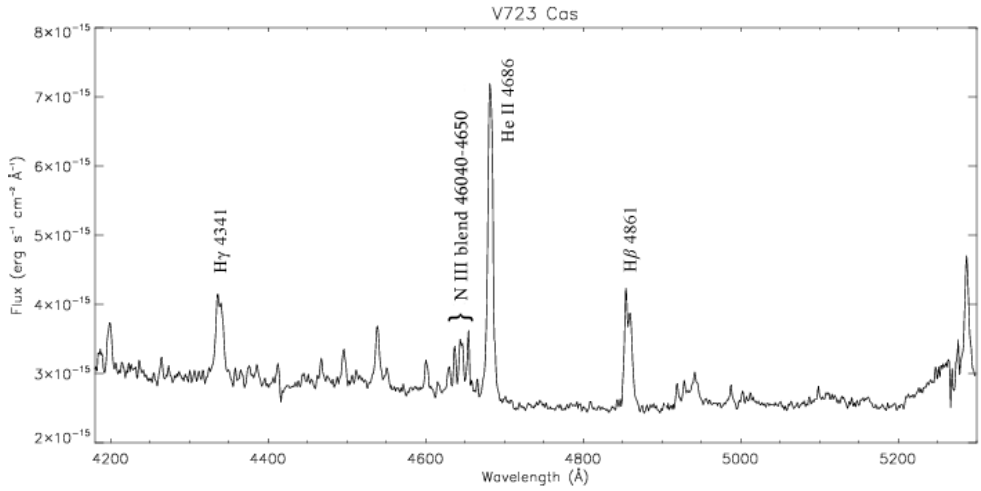

Figure 2.1 An example spectrum of V723 Cas with identifications of major emission line features in the spectral range of our observations.

2.1 He II λ4686

The He II line at λ4686 is the strongest line in the observed spectral range and exhibits a change in normalized intensity over the 16.6 hour period that can be attributed to the changing level of the underlying continuum flux (Figure 2.3). There is also a subtle but apparent asymmetry between the blue and red sides of the profile that changes over time, though it is unclear at this point how much of this may only be noise.

2.2 Hβ λ4861

Hβ is the second strongest line in the observed range and like the He II line it also shows a variability in intensity consistent with the changes in intensity. The double-peaked nature of the profile, however, is vastly more pronounced, especially near optical maximum (Figure 2.4). The intensity difference between the two peaks varies with the strongest discrepancy occurring near a phase of 0.5 when the blue-ward peak is stronger than the red-ward peak.

Although another hydrogen recombination line, Hγ, is present in the spectra, it is often too weak to provide confidence in any modeling of it and in some cases lies too close to faults in the detector causing artifacts in the data. Because of these issues, we

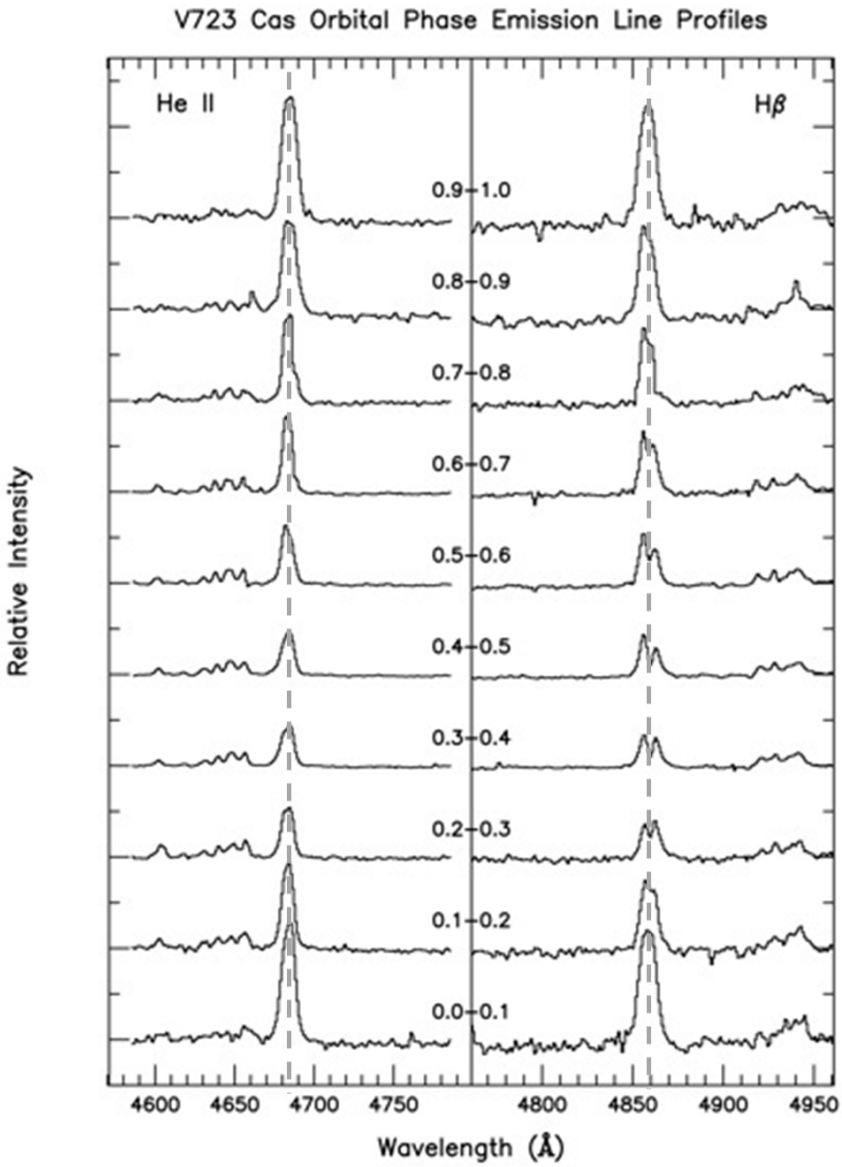

Figure 2.2 Stacked spectra of He II λ4686 (*left*) and Hβ (*right*). Dashed vertical lines have been added to guide the eye in bringing out the radial velocity variations and do *not* correspond to the rest wavelengths of the lines.

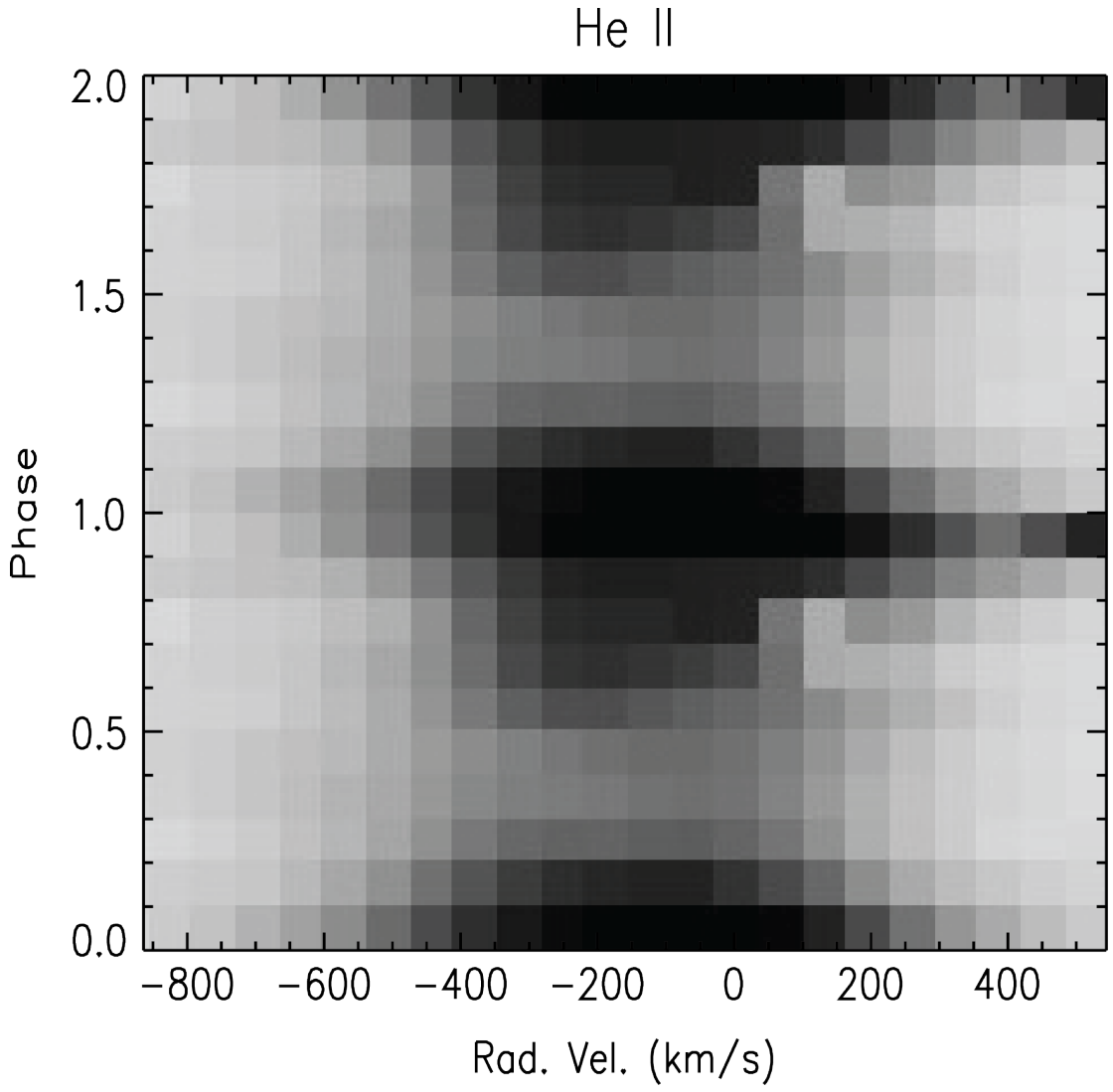

Figure 2.3 Trailed spectrogram of the continuum-normalized He II emission line profile averaged into 10 bins as a function of the orbital phase. The data are repeated over two cycles for clarity.

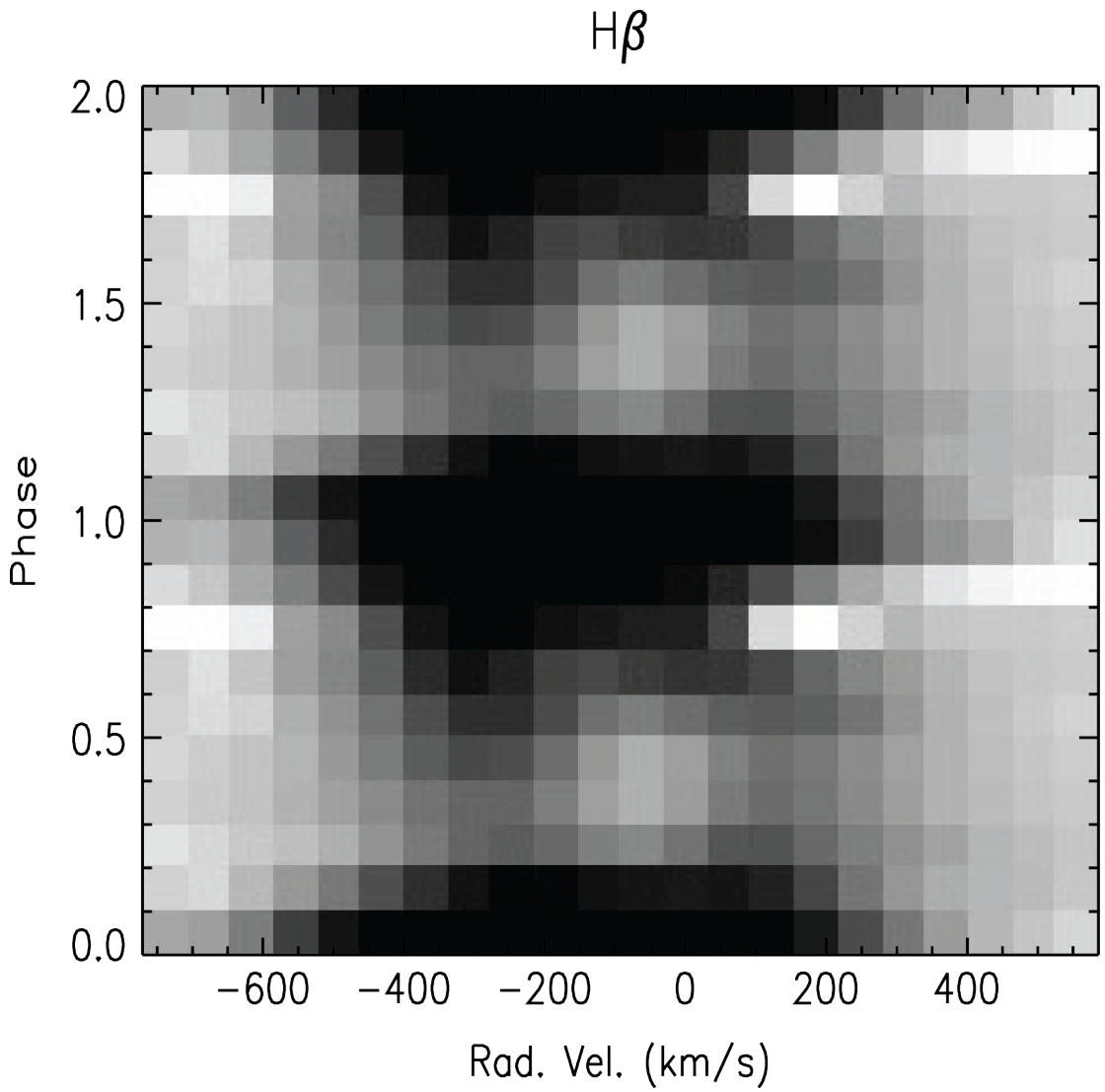

Figure 2.4 Trailed spectrogram of the continuum-normalized Hβ profile averaged into 10 bins as a function of the orbital phase. The data are shown repeated over two cycles for clarity.

opted to focus solely on the Hβ line.

2.3 Bowen Fluorescence Lines

A blend of four lines exists blue-ward of the He II λ4686 line in the $\lambda\lambda$4640–4650 region (see Figure 2.1). These lines are likely to be caused by the Bowen fluorescence mechanism of the species N III and O III, [McClintock et al., 1975]. This process results from a resonance between λ304 lines of He II and O III coupled with another resonance at λ374 between O III and N III (Figure 2.5) where Doppler broadening is greater than the small separation between the exact transition wavelengths. Although this resonance occurs in the ultraviolet wavelengths powered by the radiation field of the hot WD, a small percentage of the light re-radiates through pathways that result in the optical wavelength emissions. As with the more prominent lines, the Bowen blend also exhibits variability across the 16.6 hour orbital period. The lines are strongest at intermediate phases near photometric maximum and all but disappear near photometric minimum (as opposed to the He II and Hβ lines). This suggests that they may be tied to the source of the broadband continuum light. A small radial velocity shift is evident on visual inspection, with detailed analysis presented in Section 4.3.

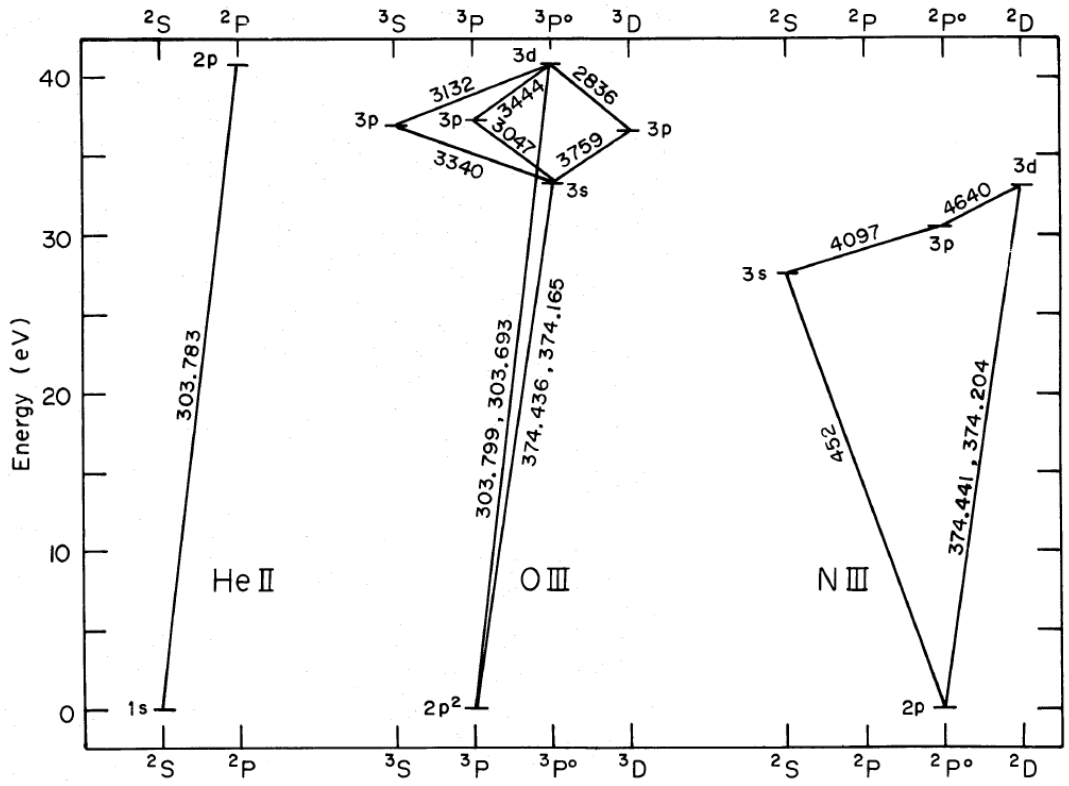

Figure 2.5 A Grotrian diagram of the atomic energy level transitions involved in the Bowen fluorescence mechanism that results in optical emission of O III and N III. (figure from McClintock et al. [1975]).

Chapter 3

Model Fits to the V723 Cas Spectral Lines

I have fit two models to the data, each with their own physical motivations:

The first model to the data is to use two overlapping Gaussian components fit using the deblending function of the IRAF[1] task *splot*. This is perhaps the simplest model to reconcile the double-peaked profiles: each Gaussian in this situation represents an independent emission region, the center and width of which are a result of its position in the binary system and the local conditions there, namely the Maxwell-Boltzmann velocity distribution associated with the local temperature (it is expected that the lines should be thermally dominated given the high temperatures). The double-peaked nature then arises simply as an overlapping of these two independent components. If one component originates on the WD and the other from the donor star, velocity measurements could be used in conjunction with Newton's laws of motion to determine the mass ratio of the two stars, helping to pin down the unknown mass of V723 Cas. The errors generated by *splot* are estimated using a Monte Carlo technique of fitting the lines N times with slightly altered initial conditions based on the original user input. For these data, $N = 100$ was used. The separation in the He II line is small, therefore I additionally fit only a single Gaussian component (i.e. a null amplitude for the second component) as

[1] IRAF is distributed by the National Optical Astronomy Observatory (NOAO), which is operated by the Association of Universities for Research in Astronomy (AURA) under cooperative agreement with the National Science Foundation.

an alternative explanation.

The second model to the data uses a Gaussian superimposed on a naturally double-peaked accretion disk profile (see Figure 3.1), fit using an IDL^{TM} routine that follows the methods described by Smak [1981]. Accretion disk emission lines are double-peaked due to one side of the disk moving toward the observer and the other side of the disk moving away, both viewed simultaneously since the disk itself is not spatially resolved due to the distance to the system. A more detailed description of the nature of accretion disk line profiles can be found in Horne and Marsh [1986]. This enables one to test whether the system is, in fact, undergoing renewed accretion. This method assumes that the accretion disk has an intrinsic radial density profile of emitting particles of $f(r) \propto r^{-\alpha}$, where a value of $\alpha \approx 2$ is appropriate for most observed disks in novae, and fits the resulting theoretical profile to the data via χ^2 minimization. Table 3.1 contains a list of all parameters fit by the model. The theoretical profile is then convolved with a Gaussian profile to match the instrumental resolution of the B&C Spec and Modspec instruments ($\sim$2Å) and this smoothed profile is fit to the data. We initially ran the fit with all parameters allowed to vary to explore the disk properties. Subsequent runs then assumed the values of $\alpha = 2$, $r_1/r_2 = 0.12$ and $u_2 = 180$ km s^{-1} and used the values of the other parameters as initial guesses to further refine the results. Errors from this method are determined by holding all parameters constant but one and examining the effect on the χ^2 value, then propagating the errors in the output parameters to those of physical interest.

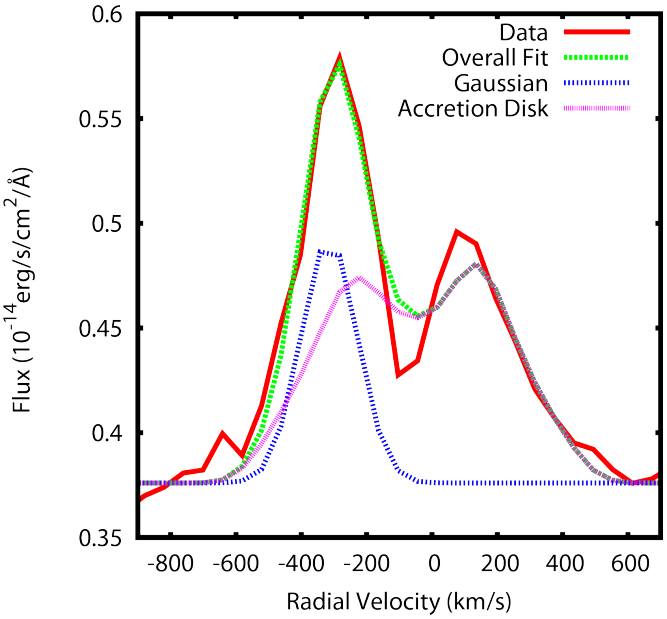

Figure 3.1 An example of the accretion disk model fit to the data. The red line represents the actual data, the purple line shows the contribution of the accretion disk, the blue line shows the contribution of the Gaussian, and the green line is the combination of both components.

Table 3.1. Accretion Disk Model Parameters

Symbol	Explanation of parameter
I_0	Intensity of the disk component
α	Power law index of the radial density profile
r_1/r_2	Ratio of the inner and outer disk radii
u_2	Velocity at the outer edge of the disk
λ_0	Centroid of the disk component
F_0	Continuum flux level
F_1	Slope of the continuum flux (set to zero for all runs)
I_G	Intensity of the Gaussian component
σ_G	Width of the Gaussian component
λ_G	Centroid of the Gaussian component

Chapter 4

Analysis

4.1 He II Results

Our accretion disk model did not converge on a solution when applied to the He II λ4686 feature and we thus fit it initially only using the double-Gaussian model. The radial velocities and peak intensities of the two fit components are plotted in Figure 4.1. In a few cases, the intensity of one component is near or consistent with zero casting doubt on the existence of two distinct components, so we also performed a single-Gaussian fit to the line (Figure 4.2) which—as with the two-Gaussian model—does not show an obvious pattern in its radial velocity curve that can be fit by a simple function. The single component fits left noticeable residuals, yet no trend was evident in these either.

4.2 Hβ Results

Fits to the Hβ line using the accretion disk model are shown in Figure 4.3. There is an apparent radial velocity trend that fits the period of the Goranskij et al. [2007] ephemeris, with the accretion disk component in near anti-phase to the Gaussian component, though there is a phase offset between the two of $\sim$ 0.1–0.15.

A different pattern emerges when two Gaussians are used to fit the data, and only one component displays a sinusoidal radial velocity curve of amplitude 94$\pm$5 km s^{-1}(Figure 4.4) while the second component stays relatively stationary over the 16.6 hour orbital period (Figure 4.5). Although the moving component appears to have the correct phasing for

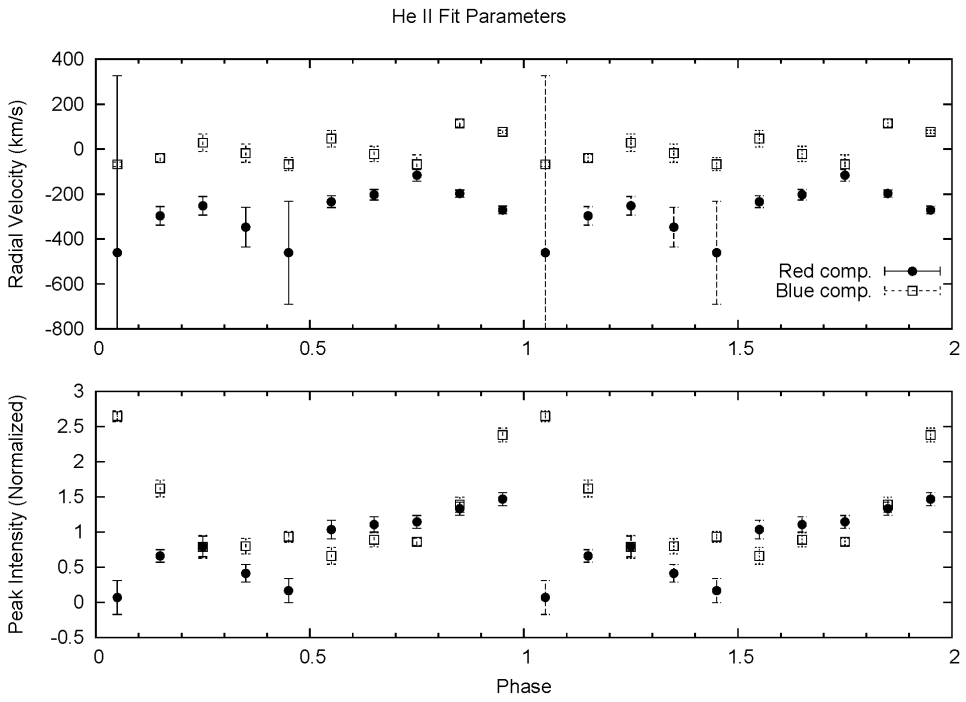

Figure 4.1 Top: Radial velocity as a function of orbital phase of the He II emission line. Bottom: Peak intensity of each component in the fit. Closed symbols indicate the red component and open symbols represent the blue component. Error bars are the 1-σ uncertainties from the output of *splot*.

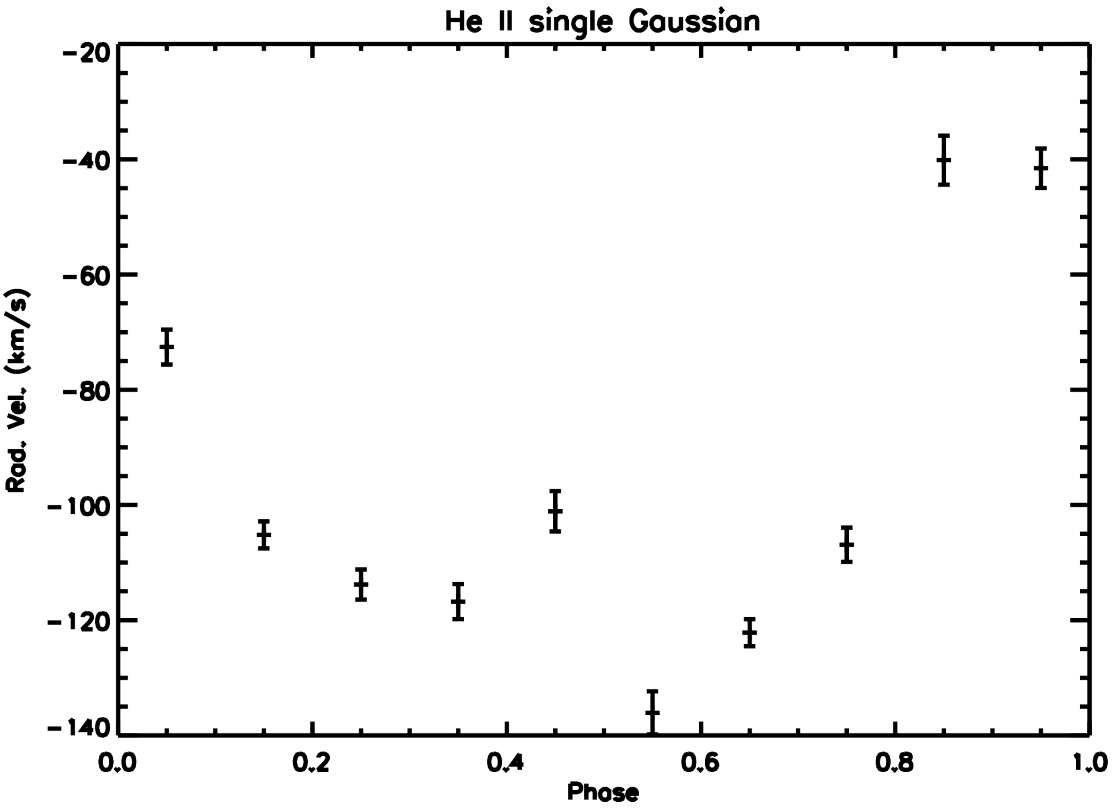

Figure 4.2 Gaussian fits to the He II line using only a single component. No attempt was made to fit a function to the data points, as no simple function will replicate the distribution. Error bars are the 1-σ uncertainties from the output of *splot*.

the period, the systemic velocity does not match, being redshifted by 106 ± 3 km s^{-1} rather than blueshifted as found in all other fits. There is also the possibility that one of the components is not Hβ, but contamination from the nearby He II λ4859 line.

4.3 Bowen Fluorescence Results

We fit the Bowen fluorescence lines with a single Gaussian to each of the four visible peaks using the IRAF task *splot*. After an initial fitting to each line allowing each component to have an independent position we found the components to share a common radial velocity and thus fixed the relative positions of the components in subsequent fits, the results of which are shown in Figure 4.6. No data exists at phases 0.05, 0.85, or 0.95 due to the disappearance of the lines at those times. Applying a least squares fit, we find a projected amplitude of $v_2 \sin i = 70 \pm 8$ km s^{-1} for the Bowen blend with a period consistent with that reported by Goranskij et al. [2007] to a factor of 1.01 ± 0.03 and with no detected phase offset within the errors (0 ± 0.03).

4.4 Discussion

In the accretion disk model of Hβ, the radial velocities are at their maximum amplitude from the apparent systemic velocity near photometric maximum. If the light curve is interpreted as arising from an irradiated face of the secondary star, this behavior is 90 degrees out of phase from what one would expect (maximum light should correspond to zero radial velocity as the orbital motion of the system components would be perpendicular to the line of sight when the irradiated side of the secondary is facing us). Similarly, the accretion disk is also out of phase from our expectation as it should trace the motion of the central WD which would also have zero radial velocity at maximum and minimum light. It is possible that the measured radial velocities are correct and it is only the interpretation of the light curve that is flawed, but higher fidelity data is needed to make that distinction.

Does any of the emission arise in the nova ejecta? Lyke and Campbell [2009] resolved the morphology of the ejecta shell for several atomic species in the near-IR, but the hydrogen recombination Brγ line still only appears as essentially a point source with

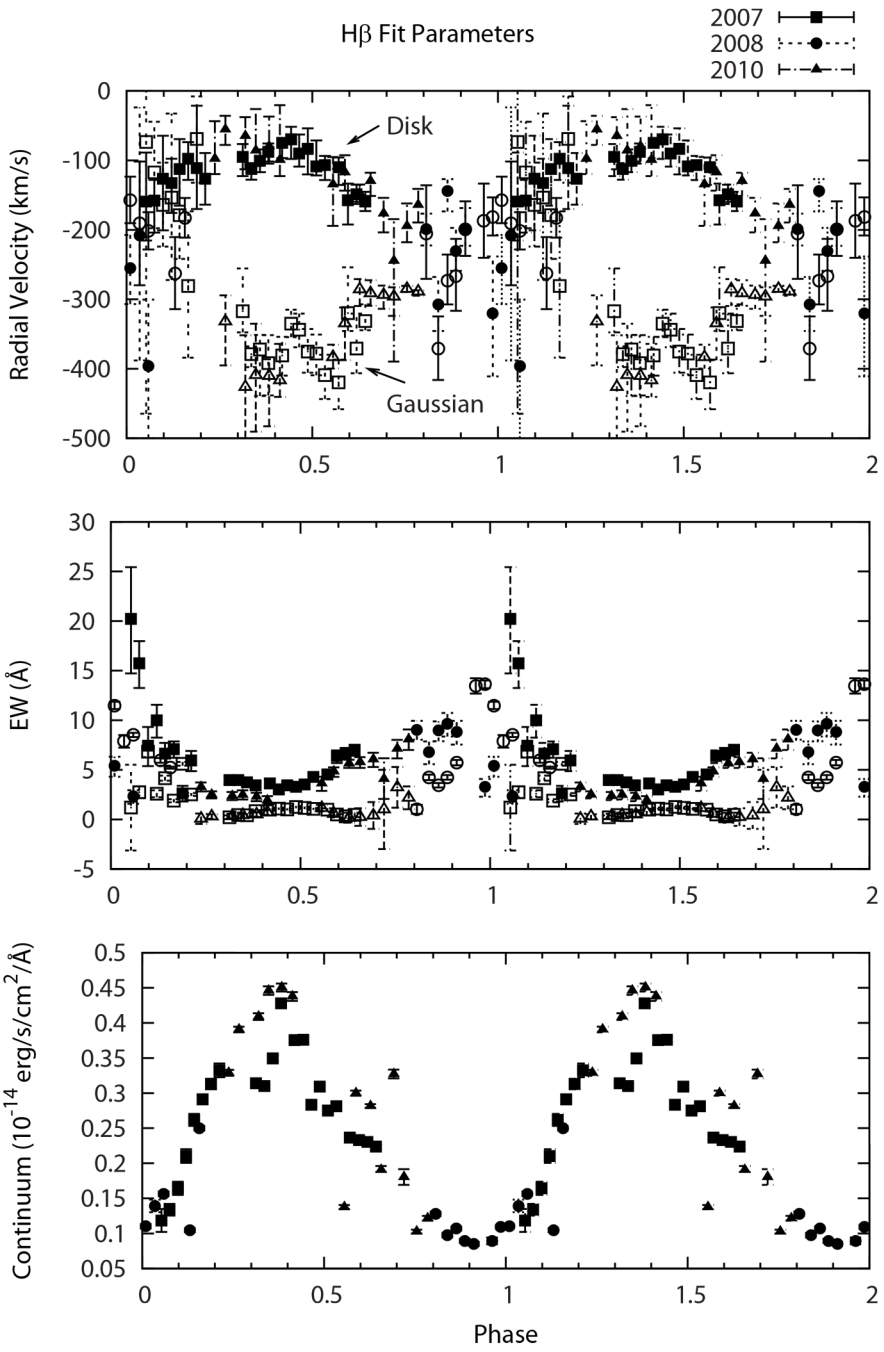

Figure 4.3 Fits to the Hβ emission line using the accretion disk model (closed symbols) with a superimposed Gaussian (open symbols). Top: radial velocity, Middle: equivalent width, Bottom: continuum level. Error bars are the 1-σ uncertainties from the χ^2 minimization of our IDL^{TM} routine.

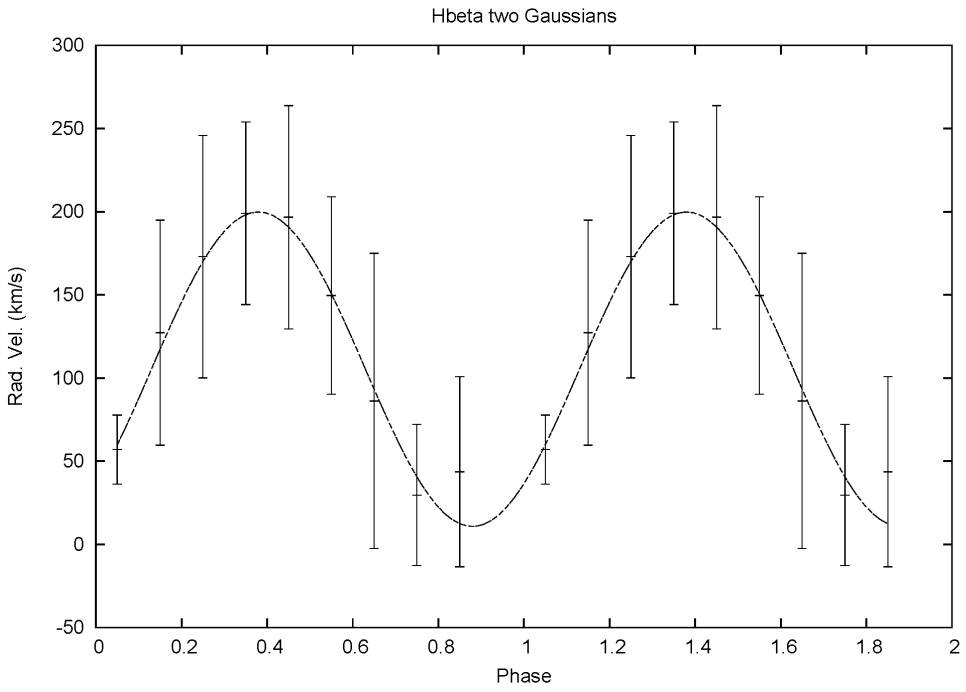

Figure 4.4 Radial velocity curve of one component of the double-Gaussian model fit to Hβ. A sine wave modulation is detected, but it is redshifted, compared to all other measurements indicating a blueshift. Error bars represent the 1-σ uncertainties reported by *splot*.

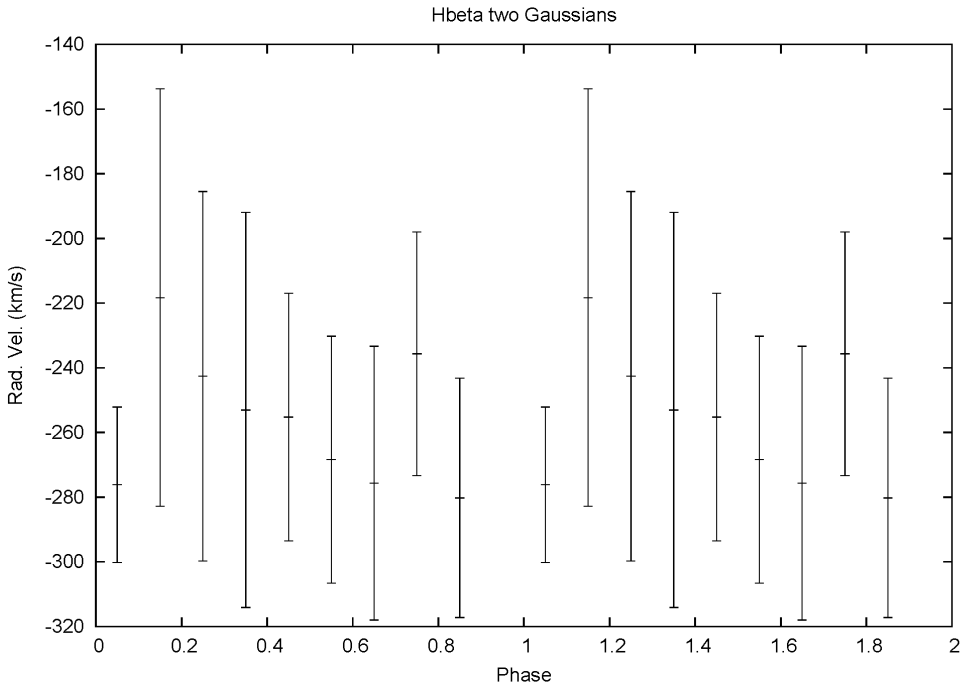

Figure 4.5 Radial velocity curve of the second component of the double-Gaussian model fit to Hβ. No radial velocity trend is distinguishable. Error bars represent the 1-σ uncertainties reported by *splot*.

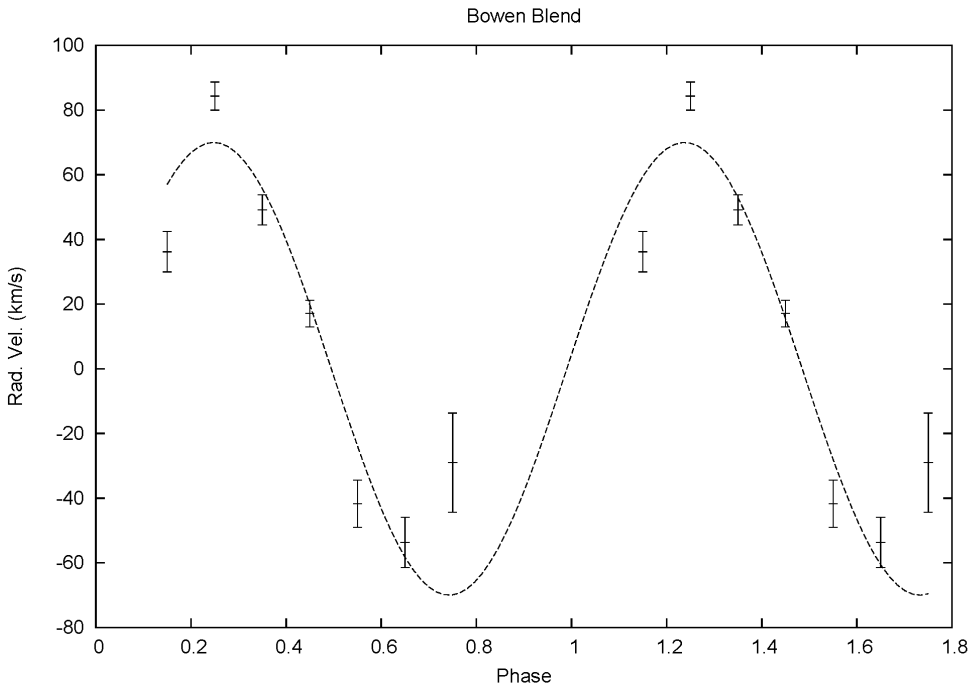

Figure 4.6 Radial velocity curve for the Bowen emission blend blueward of He II. Measurements are absent at phases 0.05, 0.85, and 0.95 due to the disappearance of the lines at those times. The systemic velocity is not included in this figure. Error bars represent the 1-σ uncertainties reported by *splot*.

limited extended emission. There is no reason to suspect other hydrogen recombination lines (such as Hβ) would be different. They do, however, measure an expansion velocity of $v_r = 443.3 \pm 12.0$ km s^{-1}, defined as the separation between the red- and blue-shifted peaks, that is in rough agreement with the separation seen in our Hβ data ($v_r = 360 \pm 60$ km s^{-1}). If the Hβ emission truly is from the ejecta, it is then unclear what could be causing the observed changes over the orbital period.

He II, despite its strength, has proved difficult to model and interpret. A lack of clear separation in the line profile makes it unlikely it arises in either an accretion disk or the ejecta. Observations at a higher spectral resolution are needed to confirm any structure, but would need to be performed on a larger telescope to be able to take short enough integration times to avoid velocity smearing of the line. He II λ4686 emission has been observed in other X-ray binary sources and found to originate near the compact primary [Steeghs and Casares, 2002]; however, we reiterate that radial velocity measurements from our data fail to show a significant trend over the orbital period. If the emission were to arise from a small subsection of an accretion disk, we may not detect a clear signal due to: 1) our observations being carried out over 3 years and; 2) our necessarily long integration times to achieve enough signal-to-noise. Given infinite spectral and temporal resolution, one might expect to see the superposition of two periods: the orbital period of the binary and the period of rotation for that point in the disk around the WD.

In addition to the strongest lines, the Bowen fluorescence lines blue-ward of He II λ4686 provide a useful diagnostic. These lines have been previously attributed to irradiation of the face of the secondary star in other X-ray systems [Steeghs and Casares, 2002]. Moreover, the negligible phase shift of our radial velocity curve and disappearance of the lines surrounding phase 0 is consistent with inferior conjunction of the secondary coinciding with the photometric minimum, when the heated face of the secondary star is facing away from Earth. Phase 0.5 would then be superior conjunction, when the heated surface faces our line of sight and we are able to observe the fluorescence lines. Thus we associate these lines with the mass donor and ascribe to it the radial velocity of $v_2 \sin i = 70 \pm 8$ km s^{-1} found in Section 4.3. Unfortunately our data have not shown another line to be in anti-phase with the Bowen blend, and we cannot make a direct constraint on the mass ratio of the V723 Cas system at present.

Chapter 5

Conclusion

We find variability in the emission line profiles and radial velocities of He II λ4686 and Hβ λ4861 of the classical nova V723 Cas over its orbital period of 16.6 hours. He II, while the overall stronger of the two lines, does not exhibit a clear separation between possible components and may only arise from a single region of emission. Radial velocity measurements of He II failed to reveal a discernible trend and thus the location of the emission region remains a mystery. Hβ shows a well-separated double peaked profile, with a variable intensity ratio between the two peaks. We posit that this is either due to: 1) an accretion disk which creates a naturally double-peaked profile superimposed with a thermally dominated component from another region of emission or; 2) two separate regions of thermally dominated emission that superimpose to create the double-peaked structure without an accretion disk. We have been unable with the current dataset to distinguish between these options and in both cases there may be contamination of the Hβ emission by He II λ4859 complicating the fits.

We have identified lines blue-ward of He II λ4686 as occurring from the Bowen fluorescence mechanism [McClintock et al., 1975] and associate these lines with the irradiated face of the secondary star in the V723 Cas system and having a radial velocity of $v_2 \sin i = 70 \pm 8$ km s^{-1}. Using the value $i = 62^\circ$ [Lyke and Campbell, 2009] this de-projects to a true velocity of $v_2 = 79 \pm 9$ km s^{-1}. A detection of lines originating from the WD primary would enable a direct measurement of the mass ratio of the two stars, however this was not possible in the current study. White dwarfs typically have nearly featureless or weak featured spectra in the optical range, so observations in

other wavelengths such as ultraviolet (Lyman series) or infrared (Brackett and Paschen series) may be necessary. A conclusive detection of an accretion disk line could also be used as a proxy to the white dwarf since the disk shares the bulk motion of the star it surrounds. Nevertheless, the measurement that was made provides compelling though not conclusive evidence for the situation where the heating of the secondary star in V723 Cas drives a higher mass loss rate which in turn provides a constant stream of fuel powering the X-ray emission from steady nuclear reactions of the surface of the WD.

Several approaches could strengthen these results and answer still other questions this study was not able to achieve. My use of 2 meter class telescopes was a limiting factor to the observations: to get a higher signal-to-noise spectrum, one can increase the exposure time per image. However this leads to smearing of the data in the time domain preventing us from seeing the desired changes over the orbital period. The most obvious way to overcome this shortfall would be to use a larger telescope, such as the MMT or Large Binocular Telescope observatories of which the University of Minnesota has access to through the Large Binocular Telescope Consortium.

Time allocation on larger observatories is, however, more stringent and it is more difficult to acquire the necessary time to make regular, repeated observations. Here we may turn to two other possible techniques. Doppler tomography can use the data already in hand in a different way to reconstruct a 2-dimensional velocity map of the system [Marsh and Horne, 1988]. This may help eliminate the ambiguity to the fits and pinpoint where the emission of the spectral features is originating, especially for the poorly resolved He II line. Tomography makes no assumptions of a model and therefore its results would be fairly robust. The results of the tomography could be used to formulate a new model for fitting the individual spectra and extract a more accurate radial velocity curve.

Another possibility would be to take new observations with a spectropolarimeter, which is a combination spectrograph and polarimeter. Light reflected by dust grains in circumstellar ejecta will tend to be polarized by the elongated, non-spherical shapes of the grains. If a certain spectral feature appears stronger in one polarization state than another, this could be a strong indication that the emission is being generated in the ejecta rather than from deeper in the interior of the binary system.

This study has also focused only on the emission lines of He II λ4686 and Hβ

λ4861: additional emission lines can be investigated, most notably the other lines of the hydrogen Balmer series, i.e. Hα λ6563 and Hγ λ4341. All of these lines, including those of this study, can also benefit from increased spectral resolution in addition to any larger telescope use, etc. This would reduce the radial velocity errors on any given measurement simply due to having a finer sampling.

All of these techniques are, of course, nonexclusive to V723 Cas itself and can be applied to any other target that warrants similar study. The CNe HR Del and V458 Vul share some similarities to V723 Cas in their light curve evolution and are therefore prime candidates for future observation.

References

D. Chochol and T. Pribulla. Photometric Study of Nova CAS 1995. *Contributions of the Astronomical Observatory Skalnate Pleso*, 27:53, April 1997.

A. Evans, R. D. Gehrz, T. R. Geballe, C. E. Woodward, A. Salama, R. A. Sanchez, S. G. Starrfield, J. Krautter, M. Barlow, J. E. Lyke, T. L. Hayward, S. P. S. Eyres, M. A. Greenhouse, R. M. Hjellming, R. M. Wagner, and D. Pequignot. Infrared Space Observatory and Ground-Based Infrared Observations of the Classical Nova V723 Cassiopeiae. *AJ*, 126:1981–1995, October 2003. doi: 10.1086/377618.

V. P. Goranskij, N. A. Katysheva, A. V. Kusakin, N. V. Metlova, T. M. Pogrosheva, S. Y. Shugarov, E. A. Barsukova, S. N. Fabrika, N. V. Borisov, A. N. Burenkov, A. G. Pramsky, E. A. Karitskaya, and A. Retter. Photometric and spectroscopic study of nova Cassiopeiae 1995 (V723 Cas). *Astrophysical Bulletin*, 62:125–146, June 2007. doi: 10.1134/S1990341307020046.

K. Hirosawa, M. Yamamoto, S. Nakano, T. Kojima, M. Iida, A. Sugie, S. Takahashi, and G. V. Williams. Nova Cassiopeiae 1995. *IAU Circ.*, 6213:1, August 1995.

K. Horne and T. R. Marsh. Emission line formation in accretion discs. *MNRAS*, 218: 761–773, February 1986.

A. Kovetz and D. Prialnik. CNO abundances resulting from diffusion in accreting nova progenitors. *ApJ*, 291:812–821, April 1985. doi: 10.1086/163117.

M. Livio. Classical novae and the extragalactic distance scale. *ApJ*, 393:516–522, July 1992. doi: 10.1086/171524.

J. E. Lyke and R. D. Campbell. The Distance and Morphology of V723 Cassiopeiae (Nova Cassiopeia 1995). *AJ*, 138:1090–1100, October 2009. doi: 10.1088/0004-6256/138/4/1090.

T. R. Marsh and K. Horne. Images of accretion discs. II - Doppler tomography. *MNRAS*, 235:269–286, November 1988.

J. E. McClintock, C. R. Canizares, and C. B. Tarter. On the origin of 4640-4650 A emission in X-ray stars. *ApJ*, 198:641–652, June 1975. doi: 10.1086/153642.

J.-U. Ness, G. Schwarz, S. Starrfield, J. P. Osborne, K. L. Page, A. P. Beardmore, R. M. Wagner, and C. E. Woodward. V723 CASSIOPEIA Still on in X-Rays a Bright Super Soft Source 12 Years after Outburst. *AJ*, 135:1328–1333, April 2008. doi: 10.1088/0004-6256/135/4/1328.

H. Ritter and U. Kolb. Catalogue of cataclysmic binaries, low-mass X-ray binaries and related objects (Sixth edition). *A&AS*, 129:83–85, April 1998. doi: 10.1051/aas:1998175.

G. J. Schwarz, J.-U. Ness, J. P. Osborne, K. L. Page, P. A. Evans, A. P. Beardmore, F. M. Walter, L. A. Helton, C. E. Woodward, M. Bode, S. Starrfield, and J. J. Drake. Swift X-Ray Observations of Classical Novae. II. The Super Soft Source Sample. *ApJS*, 197:31, December 2011. doi: 10.1088/0067-0049/197/2/31.

J. Smak. On the Emission Lines from Rotating Gaseous Disks. *Acta Astronomica*, 31: 395, 1981.

S. Starrfield, F. X. Timmes, C. Iliadis, W. R. Hix, W. D. Arnett, C. Meakin, and W. M. Sparks. Hydrodynamic Studies of the Evolution of Recurrent, Symbiotic and Dwarf Novae: the White Dwarf Components are Growing in Mass. *Baltic Astronomy*, 21: 76–87, 2012.

D. Steeghs and J. Casares. The Mass Donor of Scorpius X-1 Revealed. *ApJ*, 568: 273–278, March 2002. doi: 10.1086/339224.

C. E. Woodward and S. Starrfield. Recent observational and theoretical studies of the

classical nova outburst. *Canadian Journal of Physics*, 89:333–343, April 2011. doi: 10.1139/p11-010.

Appendix A

Glossary and Acronyms

Care has been taken in this thesis to minimize the use of jargon and acronyms, but this cannot always be achieved. This appendix defines jargon terms in a glossary, and contains a table of acronyms and their meaning.

A.1 Glossary

- **Binary Phase** – A method of expressing the orbital configuration of a binary system as a fraction of the orbital period with respect to an arbitrary zero point, often the point of minimum brightness of the light curve. Ex. A binary phase of 0.2 in a system with an orbital period of 10 hr means 2 hr after the chosen zero point.
- **Chandrasekhar Limit** – The theoretical upper mass limit for a white dwarf star of approximately $1.4M_{\odot}$ where the gravitational force exceeds the electron degeneracy pressure. Electron degenerate matter with a mass greater than this limit will collapse into either a neutron star supported by neutron degeneracy pressure or a black hole.
- **Classical Nova** (**CN - singular; CNe - plural**) – An explosion on the surface of a white dwarf star as a result of a runaway thermonuclear reaction triggered via mass transfer in a binary star system.

- **CNO Cycle** – A method of fusion that uses carbon, nitrogen, and oxygen as catalysts to fuse hydrogen into helium.
- **Electron Degeneracy Pressure** – A pressure that opposes the force of gravity in a white dwarf star due to electrons being unable to occupy the same quantum mechanical energy state, i.e. the Pauli exclusion principle.
- **Lagrangian Point** – One of five points in the gravitational potential of a binary system where the gravitational pulls of the two masses balance out on a third object of negligible mass to co-rotate with the system. The most important of these points in novae is the inner Lagrangian point, L_1, located between the two larger masses.
- **Light Curve** – A plot of an object's brightness over time.
- **Main Sequence (MS)** – The stage of stellar evolution in which the majority of a star's life is spent and the primary source of energy is the fusion of hydrogen into helium in its core.
- **Roche Lobe** – A region of space surrounding a star in a binary system where matter is bound to that star. Material outside of the Roche lobe can potentially escape the gravitational pull of the star.
- **Roche Lobe Overflow** – A method of mass transfer in a binary system where if one star overfills its Roche lobe, material can flow through the inner Lagrangian point and accrete onto the other star.
- **Standard Candle** – An object of known luminosity that can be used to measure distance by comparing the luminosity to the observed apparent brightness.
- **Type Ia Supernova** – A type of supernova explosion that is thought to result from a white dwarf exceeding the Chandrasekhar limit. In contrast to a classical nova, the entire star is disrupted. Because of the consistency of the mass limit, they may be used as 'standard candles' to determine extragalactic distances.
- **White Dwarf** (**WD**) – The inert, electron degenerate core of a low-mass star left over after the star ejected its outer layers.

A.2 Acronyms

Table A.1: Acronyms

Acronym	Meaning
AURA	Association of Universities for Research in Astronomy
CN	Classical nova
CNe	Classical novae
IRAF	Image Reduction and Analysis Facility
MMRD	Maximum magnitude–rate of decline relationship
MS	Main sequence
NOAO	National Optical Astronomy Observatory
RN	Recurrent nova
RNe	Recurrent novae
SN	Supernova
SNe	Supernovae
SSS	Super soft X-ray source
TNR	Thermonuclear runaway
WD	White dwarf